ACS chemical biology

ARTICLES

pubs.acs.org/acschemicalbiology

Identification of a Polyoxometalate Inhibitor of the DNA Binding Activity of Sox2

Kamesh Narasimhan,[†,‡] Shubhadra Pillay,[§] Nor Rizal Bin Ahmad,[∥] Zsolt Bikadi,[⊥] Eszter Hazai,[⊥] Li Yan,[§] Prasanna R. Kolatkar,[†,‡] Konstantin Pervushin,[§] and Ralf Jauch[†,*]

[†]Laboratory for Structural Biochemistry, Genome Institute of Singapore, Singapore 138672

[‡]Department of Biological Sciences, National University of Singapore, Singapore 117543

[§]School of Biological sciences, Nanyang Technological University, Singapore 637551

[∥]High Content Screening Lab, Genome Institute of Singapore, Singapore 138672

[⊥]Virtua Drug Research and Development Ltd., Budapest 1015, Hungary

Supporting Information

ABSTRACT: Aberrant expression of transcription factors is a frequent cause of disease, yet drugs that modulate transcription factor protein−DNA interactions are presently unavailable. To this end, the chemical tractability of the DNA binding domain of the stem cell inducer and oncogene Sox2 was explored in a high-throughput fluorescence anisotropy screen. The screening revealed a Dawson polyoxometalate ($K_6[P_2Mo_{18}O_{62}]$) as a direct and nanomolar inhibitor of the DNA binding activity of Sox2. The Dawson polyoxometalate (Dawson-POM) was found to be selective for Sox2 and related Sox-HMG family members when compared to unrelated paired and zinc finger DNA binding domains. [^{15}N,^{1}H]-Transverse relaxation optimized spectroscopy (TROSY) experiments coupled with docking studies suggest an interaction site of the POM on the Sox2 surface that enabled the rationalization of its inhibitory activity. The unconventional molecular scaffold of the Dawson-POM and its inhibitory mode provides strategies for the development of drugs that modulate transcription factors.

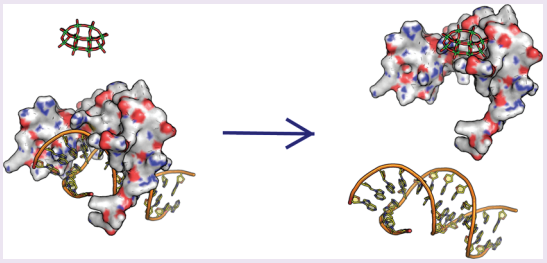

The pharmacological potential of transcription factor−DNA interactions remain untapped because DNA binding domains are generally perceived as challenging targets.[1−3] The challenge is posed because transcription factors lack the hydrophobic and deep ligand binding pockets characteristic for enzymes and cell surface receptors.[4] Instead, transcription factors possess an extended and positively charged recognition interface to dock to polyanionic DNA elements. Moreover, the DNA binding domains are often subjected to structural rearrangements upon DNA binding, whereas the ligand binding pockets of enzymes are largely preformed.[4] Despite these difficulties, several studies demonstrated that transcription factors can be directly targeted by small molecules. For example, small molecule microarrays have been employed to target yeast transcription factor subunits.[5] By using fluorescence anisotropy based screens, inhibitors of the DNA binding activity of estrogen receptor ER-α, B-zip, and Hoxa13 were identified.[6−8] Furthermore, an inhibitor of the apoptosis inducing factor (AIF) was identified using photonic crystal biosensors.[2] The structure activity relationships often remain elusive but could be established for some electrophilic compounds that inhibit zinc finger transcription factors by ejecting the coordinated Zinc ion leading to a collapse of the protein's structural integrity as shown for HIV-NCP7 and ER-α.[9,10] Other notable examples that affect DNA binding include inhibitors of c-Myc/Max, HIF (hypoxia inducible factor) and E2F.[4,11−13] Approaches wherein small molecules modulate transcription by binding to DNA sequences face the challenge of achieving target DNA specificity.[14] We chose Sox2 for our screen on the basis of its critical roles in stem cell and cancer biology. Sox2 is required for the maintenance of pluripotency and self-renewal of embryonic stem (ES) cells.[15] Consistently, knock-down of Sox2 results in the loss of the undifferentiated state.[16,17] By featuring in a cocktail of four transcription factors required for generating induced pluripotent stem (iPS) cells Sox2 gained further prominence.[18] To induce and maintain pluripotency Sox2 directly interacts with Oct4 when bound to its DNA targets mediated by a small and charged protein interaction surface.[19] The oncogenic potential of Sox2 was recognized after elevated expression levels were detected in several tumors such as lung cancer, gastric carcinoma, malignant glioma and in breast cancer.[20−22] It has therefore been hypothesized that the aberrant upregulation of Sox2 promotes tumorigenesis by stimulating self-renewal, dedifferentiation, proliferation, and cell survival reminiscent of its role in stem cell biology.[20] Indeed, Sox2 was

Received: December 30, 2010
Accepted: February 22, 2011
Published: February 23, 2011

reported to be a lineage survival oncogene in squamous cell carcinomas and was found to be highly expressed in cancer stem cells leading to myeloma.[22,23] Together, these studies suggest that Sox2 acts at the onset of carcinogenesis as well as in cancer stem cells with a high proliferative potential that are top priority targets for anticancer therapy. In the light of the importance of Sox2 in stem cell and cancer biology, we envisage small molecule inhibitors of Sox2 to have two areas of application: (i) as anticancer drugs and (ii) as tools to direct differentiation for tissue engineering.[24] DNA binding by Sox2 is mediated by a ~80 residue high mobility group (HMG) domain that binds to a consensus C(T/A)TTG(T/A)(T/A) motif.[25] Its angular inner surface binds to the minor groove of the DNA and inserts a phenylalanine-methionine wedge into DNA base pairs inducing a ~70° kink. The HMG domain consists of a three-helix bundle, exhibiting a L-shaped structure composed of flexible major and minor wings that are subject to some structural rearrangements upon DNA binding.[19,26−28] This structural flexibility may pose a challenge due to the absence of a preformed small-molecule binding pocket and context-dependent conformational adaptability. Alternatively, we hypothesized that the flexibility and "clamp"-like architecture of the Sox-HMG domain might enable it to wrap around inhibitor molecules in an induced-fit type of mechanism.

In this study, we identified a Dawson polyoxometalate as a nanomolar inhibitor of the DNA binding activity of Sox2. This binding is direct and selective for HMG domains in comparison to other DNA binding domains. We further mapped the interaction surface of Sox2 with the Dawson-POM by NMR and *in silico* docking. Together, we demonstrate that challenging molecular architectures like the DNA binding domains are tractable drug targets and propose Dawson polyoxometalates as molecular scaffolds for transcription factor inhibition.

RESULTS AND DISCUSSION

Primary Screening and Identification of a Polyoxometalate Hit. The *CCND1* gene encoding cyclin D1 is linked to breast cancer progression and upregulated by Sox2.[29] We therefore utilized Sox2 binding to the *cis*-regulatory element of *CCND1* as the basis for a fluorescence anisotropy based screen. When Sox2-HMG binds the 22bp FAM labeled *CCND1* DNA element, the larger size of the protein−DNA complex causes a slower rotation resulting in a relatively higher anisotropy (Figure 1, panel a). Addition of unlabeled competitor DNA to the complex results in complete displacement of the labeled *CCND1*-Sox2-HMG complex (Figure 1, panel b). The large signal window separating Sox2 bound and unbound DNA facilitated the upscaling of the assay into a robust high-throughput format to identify inhibitors that can disrupt Sox2-HMG DNA complex formation (Figure 2, panel a). Compound screening was carried out using the mechanistic and the challenge diversity libraries obtained from the National Cancer Institute (NCI, http://dtp.nci.nih.gov/index.html). The Mechanistic diversity library (825 compounds) is derived from 37,836 compounds that have been tested on the NCI human tumor 60 cell line and represents compounds that exhibit a broad range of growth inhibition effects. The Challenge diversity set (1364 compounds) was derived from a 140,000 compound collection to create a structurally diverse library. In total, 2,189 compounds were screened in duplicates in 384-well plates. Measurements obtained from the positive and negative control samples in each microplate were used to calculate the Z′ factor. For all microplates the Z′ factor was >0.60 (Figure 2, panel b), and replicate screens showed high reproducibility (Figure 2, panel c). Compounds with composite Z-score less than or equal to −3 and reproducibility less than −0.98 were identified as primary hits (Figure 2, panel d). This way, we identified 51 compounds as potential primary hits (Supplementary Table 1). Many hits included planar and aromatic compounds with possible DNA intercalator activity and were not analyzed further. One candidate inhibitor was a Dawson polyoxometalate $K_6[P_2Mo_{18}O_{62}]$ (NSC 622124), henceforth referred to as Dawson-POM. POMs are nanometer sized oxyanions made up of group 5 and group 6 transition metals such as molybdenum and tungsten.[30,31] Despite being anionic, large, and highly charged, POMs have a well-documented antiviral, antibacterial, and antitumorigenic property.[32] For example, HPA-23, a heteropolytungstate, was initially used in clinical trials to treat AIDS patients.[33] Although the mechanism of POM action remains largely obscure, a number of studies suggested that POMs directly inhibit proteins such as HIV-1 reverse transcriptase, *E. coli* Klenow DNA pol I, and eukaryotic DNA pol β.[32,34,35] Due to the high negative charge density it was suggested that the polyoxometalates I $[(O_3POPO_3)_4W_{12}O_{36}]^{16-}$ and II $[(O_3PCH_2PO_3)_4W_{12}O_{36}]^{16-}$ interact and compete with the DNA binding domains of HIV-1 RT and the DNA polymerases through electrostatic forces.[36] Indeed, the potential of the POM scaffold to bind to DNA binding domains was illustrated by the crystal structure of Rad51 with sodium metatungstate revealing a competitive mode inhibiting its DNA binding activity.[37] The Dawson-POM has recently been reported to selectively bind and

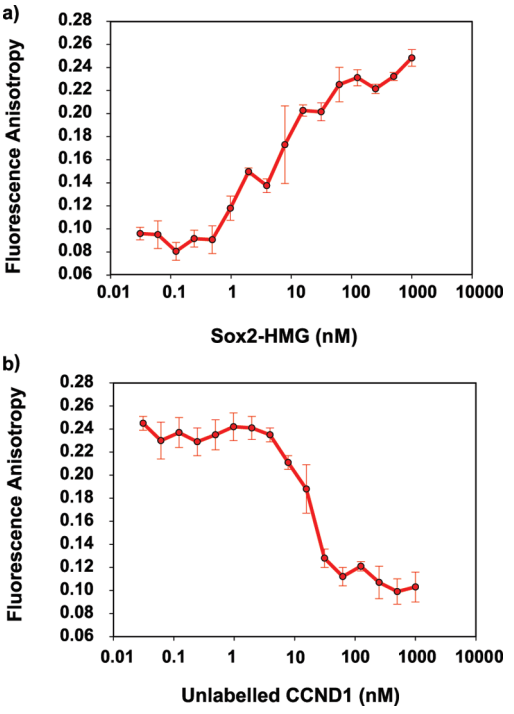

Figure 1. Fluorescence anisotropy based assay for Sox2-HMG DNA binding. (a) Binding isotherm of Sox2-HMG with 1 nM (FAM)-*CCND1*. Increasing concentrations of Sox2-HMG increases the fluorescence anisotropy indicating Sox2-HMG DNA complex formation. Data represent the average of 3 independent measurements. (b) A preformed Sox 2-HMG/(FAM)-*CCND1* complex was titrated with unlabeled *CCND1* competitor resulting in the return of anisotropy readings to the baseline.

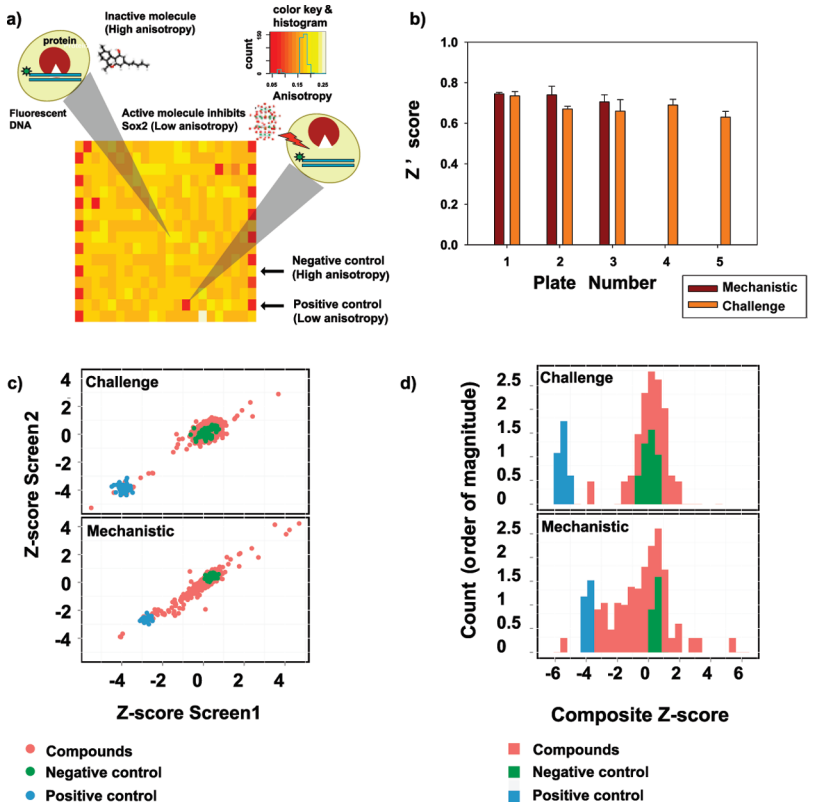

Figure 2. Fluorescence anisotropy based screen to identify inhibitors of Sox2-HMG DNA binding. (a) Assays were carried out in a 384-well microplate depicted schematically as a heatmap (color coded by anisotropy values). Compounds were added to each well, while the positive and negative controls were alternately added to the peripheral columns. (b) The dimensionless Z′ factor was used to evaluate the performance of the controls of the assay in a screening setup. The challenge diversity library required screening in five 384-well microplates, whereas the mechanistic diversity library screening was performed in three 384-well microplates. An average Z′ factor from duplicate screens (Screen 1 and Screen 2) of the challenge and mechanistic diversity libraries revealed a value above 0.6, indicating a sufficiently large signal window for robust hit identification. (c) Z-scores from duplicate screens correlate well highlighting the reproducibility of the assay. (d) Screening results are shown as histograms of composite Z-scores. Primary hits were defined as having a composite Z-score ≤ 3 and reproducibility below -0.98. Eighteen compounds from the challenge diversity and 33 compounds from mechanistic diversity were classified as primary hits.

inhibit the protein kinase CK2 and certain kinesins.[38,39] Given the inhibitory potential of POMs, we decided to further study the Sox2-HMG POM interactions.

Effect of Different POMs on Sox2-HMG DNA Binding. To compare inhibition by different POMs, various structurally diverse POMs were tested for Sox2 binding. We found that the originally identified Dawson-POM ($K_6[P_2Mo_{18}O_{62}]$) was most potent among all tested POMs (Table 1). Sodium metatungstate, known previously to competitively bind to Rad51, exhibits moderate inhibitory activity followed by the Dawson-phosphotungstate. Keggin POMs were inactive at the concentrations tested in this study. The Dawson-phosphomolybdate $[P_2Mo_{18}O_{62}]^{6-}$ is known to undergo multiple condensation-hydrolysis equilibria in solution depending on the pH and temperature.[40] For example, phospho-molybdic Dawson-type POMs like $(NH_4)_6[P_2Mo_{18}O_{62}]$ decompose into the lacunar Keggin-type anion $H_xPMo_{11}O_{39}^{(7-x)-}$, pentamolybdodiphosphate $H_xMo_5P_2O_{23}^{(6-x)-}$, phosphate, and oxomolybdate depending on the acidity-basicity of the solution.[40] However, the degradation products molybdate ($[MoO_4]^{2-}$) the phosphate ($[HPO_4]^{2-}$) and Keggin phosphomolybdate ($[PMo_{12}O_{40}]^{2-}$) were found to be insufficient to inhibit the Sox2-HMG (Figure 3, panel a and b). We therefore concluded that a structurally intact Dawson structure interacts with the Sox2-HMG.

The Dawson-POM Directly Inhibits Sox2-HMG but Not Unrelated Transcription Factors. To assess the selectivity of the Dawson-POM for the Sox2-HMG, we tested its inhibitory potential to unrelated transcription factors Pax6 and REST. Pax6 contains a bipartite paired domain and REST binds DNA via eight Cys_2/His_2 Zinc-finger domains.[41,42] Using EMSAs, we found that the Dawson-POM inhibits Sox2-HMG DNA binding with an IC_{50} value of 98.6 ± 22.1 nM, whereas the Pax6 paired domain activity is not affected by the POM even at very high concentrations (Figure 3, panels c and d). REST retains nearly all of its DNA binding activity at POM concentrations inhibiting Sox2, although some inhibition was observed at very high concentrations (Supplementary Table 2). The varying inhibition profiles of the Dawson-POM to unrelated structural classes of transcription factors suggest that the Dawson-POM is selective for certain transcription factor targets.

Next we verified that the Dawson-POM directly binds the Sox2-HMG domain. First, limited trypsin digestion of the Sox2-HMG revealed that the Dawson-POM confers sustained resistance to proteolytic digestion (Figure 4, panel a). Second, a comparison of the thermal unfolding of the Sox2-HMG domain in the absence and presence of the Dawson-POM revealed differences that can be attributed to a stabilization effect of the POM on the melting profile of Sox2-HMG. The addition of

dx.doi.org/10.1021/cb100432x |ACS Chem. Biol. 2011, 6, 573–581

Table 1. Inhibition of a Saturated Sox2-DNA Complex (~95% bound) by Different POMs Monitored by Fluorescence Anisotropy

formula	M (g mol^{-1})	residual DNA binding activity at 1 μM compound (%)	type
$K_6[P_2Mo_{18}O_{62}]$	3015	31 ± 1.5	Dawson
$K_6[P_2W_{18}O_{62}]$	4597.8	76 ± 4	Dawson
$Na_3[PW_{12}O_{40}]$	2946	91 ± 1	Keggin
$Na_3[PMo_{12}O_{40}]$	1891.2	99 ± 3	Keggin
$Na_6[H_2W_{12}O_{40}]$	2986.13	51 ± 3	metatungstate
Na_3MoO_4	120	92 ± 4	molybdate
NaH_2PO_4	205.92	99 ± 5	phosphate

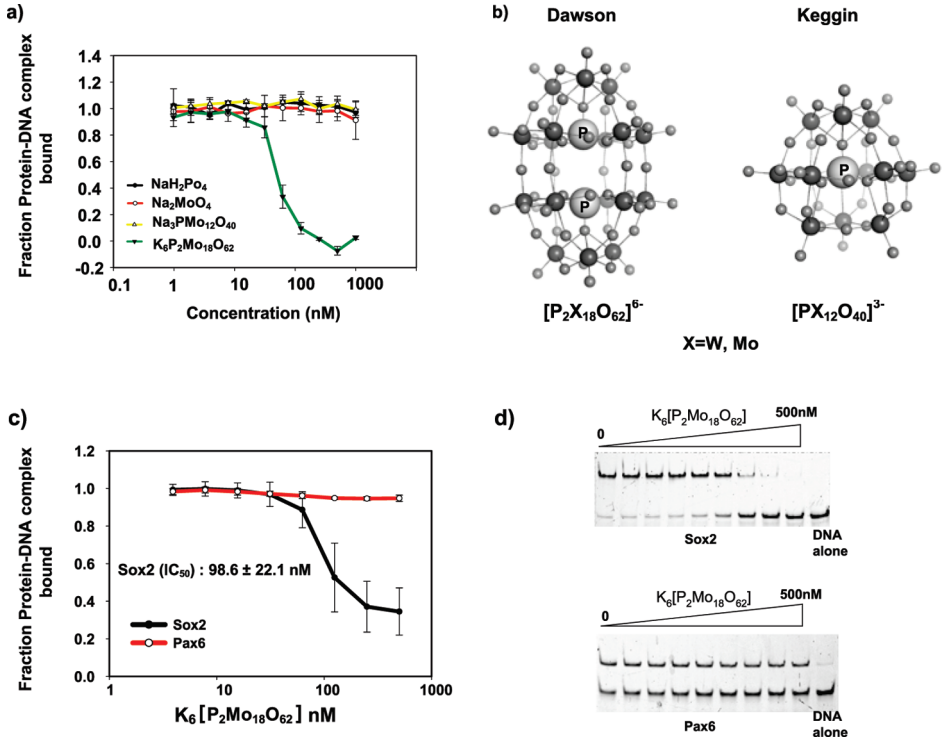

Figure 3. Effect of POM fragments on Sox2-HMG inhibition and selectivity of the Dawson-POM ($K_6[P_2Mo_{18}O_{62}]$) in disrupting protein−DNA complexes. (a) Fluorescence anisotropy assay showing that degradation products of $K_6[P_2Mo_{18}O_{62}]$, namely, the phosphate ($[HPO_4]^{2-}$), the molybdate ($[MoO_4]^{2-}$), and the Keggin phosphomolybdate ($[PMo_{12}O_{40}]^{3-}$), do not disrupt a half-saturated Sox2-HMG DNA complex. (b) Ball and stick representation of the Dawson and Keggin POMs. Small light gray spheres are oxygen atoms and the bigger dark spheres are transition metals like Mo and W. The central phosphate atoms are labeled. (c) EMSAs using varying POM concentrations show that $K_6[P_2Mo_{18}O_{62}]$ inhibits the Sox2-HMG with an IC_{50} value of 98.6 ± 22.1 nM but does not inhibit Pax6. (d) Representative EMSA experiment showing dose-dependent titrations of $K_6[P_2Mo_{18}O_{62}]$ with 40 nM Sox2-HMG and 1 nM CCND1 (~50−80% fraction bound) and 0.5 nM Pax6 and 1 nM consensus *pax6* DNA element (~50% fraction bound).

increasing concentrations of the Dawson-POM transformed the melting profile and increased the unfolding transition, suggesting that the Dawson-POM directly binds and stabilizes the Sox2-HMG domain (Figure 4, panel b).

Studies of Sox2-Dawson-POM Interaction by NMR. To understand the inhibitory mechanism and to facilitate the follow-up chemistry aimed at optimizing the selectivity and potency of the Dawson-POM, we assigned Sox2-HMG backbone resonances using TROSY spectroscopy and tracked the chemical shift perturbations in Sox2 after addition of the Dawson-POM. TROSY-line HNCA, HNCACB, and CBCAcoNH spectra were recorded using ^{13}C- and ^{15}N-labeled Sox2-HMG. Approximately 90% of the 114 residues of the Sox2-HMG construct were unambiguously assigned, with the unassigned residues predominantly located in the structurally flexible termini. Importantly, resonances stemming from residues comprising the helical core of the Sox2-HMG domain and DNA contacting residues are sufficiently dispersed and can be used for POM binding studies (Figure 5, panel a). POM binding to Sox2-HMG was monitored in a series of $[^{15}N,^{1}H]$-TROSY spectra recorded in the absence and presence of the Dawson-POM. When the Dawson-POM was added to 0.65 mM protein, backbone resonances of several residues in Sox2-HMG were significantly perturbed, indicating direct and specific interactions (Figure 5, panel a). Chemical shift perturbations were quantified by using overall weighted chemical shift values ($\Delta\delta = [\Delta\delta^2H_N + (0.2\Delta\delta N)^2]^{1/2}$) and displayed on a Sox2 model derived from the Sox2-Oct1/DNA structure (Figure 5, panel b). On the basis of distribution of the weighted chemical shift values, residues were classified into (i) those that undergo significant chemical shift changes ($\Delta\delta \geq 0.065$ ppm), (ii) those that undergo moderate chemical shift changes (0.04 ppm $\geq \Delta\delta <$ 0.065 ppm), and (iii) those with low chemical shift

dx.doi.org/10.1021/cb100432x |*ACS Chem. Biol.* 2011, 6, 573–581

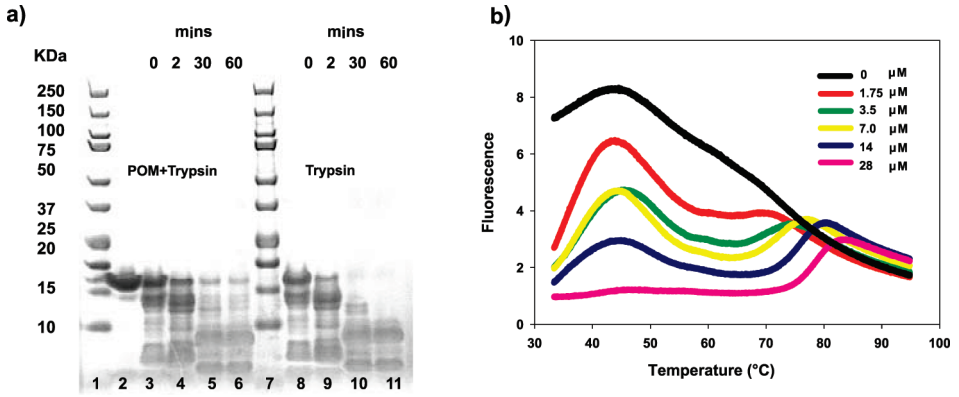

Figure 4. The Dawson-POM physically interacts with the Sox2-HMG domain. (a) Limited proteolysis reveals that interaction of Sox2 with $K_6[P_2Mo_{18}O_{62}]$ confers resistance to proteolytic digestion by trypsin. Sox2-HMG was incubated with trypsin in the presence (lanes 3−6) and absence (lanes 8−11) of the Dawson-POM. Reactions were stopped after different time points and analyzed by 4−12% SDS-PAGE. Lanes 1 and 7 contain markers, and lane 2 contains the Sox2-HMG incubated without trypsin. (b) Thermal melting profiles of Sox2-HMG monitored in the presence of sypro-orange at increasing concentrations of the Dawson-POM. As the POM concentration is increased the initially high fluorescence at lower temperatures (37−50 °C) decreases, suggesting POM-mediated stabilization.

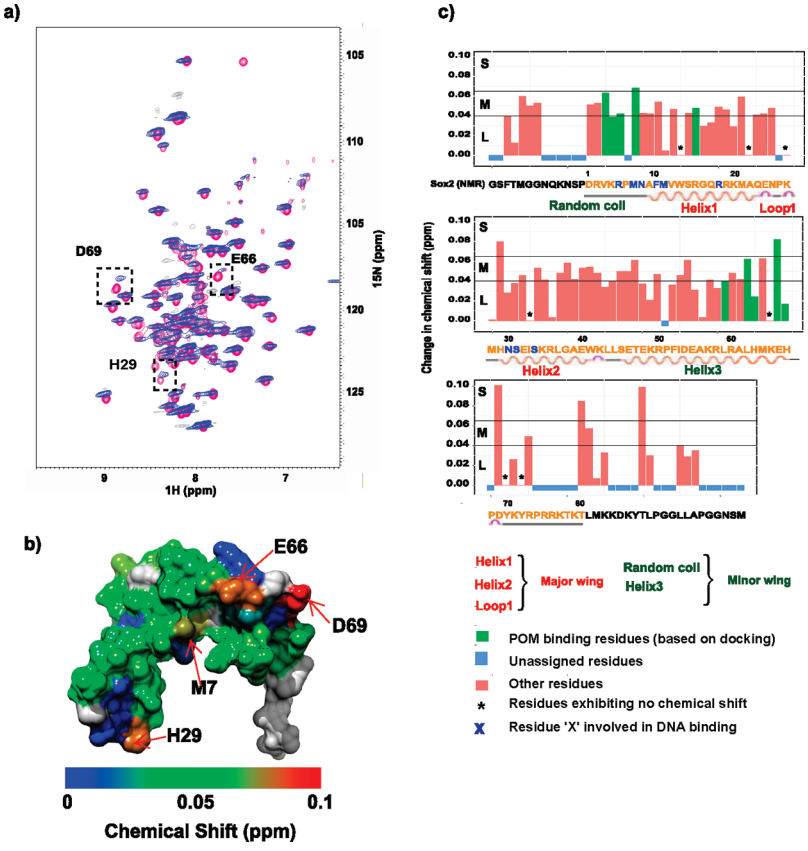

Figure 5. Interaction of Sox2-HMG with Dawson-POM analyzed by [^{15}N,^{1}H]-TROSY and docking studies. (a) Superposition of two-dimensional TROSY spectra of free Sox2 (pink) and Sox2 bound to POM (blue). Peaks that undergo significant shifts upon complex formation are highlighted. (b) The weighted change in chemical shift perturbations ($\Delta\delta = [\Delta\delta^2H_N + (0.2\Delta\delta N)^2]^{1/2}$) obtained from the [^{15}N,^{1}H]-TROSY experiments are mapped on the Sox2-HMG surface (PDB: 1GT0). Residues which are significantly shifted are labeled. The colored bar displays the extent of NMR chemical shift perturbations in ppm. Unassigned residues are colored in gray. (c) Changes in chemical shift upon POM binding is plotted as a function of the Sox2 amino acid sequence (numbered according to Sox2: PDB 1GT0). Threshold windows indicating significant (S: $\Delta\delta \geq 0.065$ ppm), moderate (M: 0.04 ppm $\geq \Delta\delta < 0.065$ ppm), and low (L: $\Delta\delta < 0.04$ ppm) chemical shift perturbations are marked with horizontal lines. Green colored bars indicate residues implicated in direct binding to POM based on docking studies. Residues that are not perturbed in TROSY experiments are indicated with an asterisk (∗). Unassigned residues are marked with a blue bar. Sox2-HMG residues involved in DNA binding are colored in blue in the one letter aminoacid sequence. Secondary structural elements are depicted and colored to indicate the corresponding major and minor wing structural domains.

dx.doi.org/10.1021/cb100432x |*ACS Chem. Biol.* 2011, 6, 573–581

changes ($\Delta\delta$ < 0.04 ppm) (Figure 5, panel c). The residues Met7, His29, Glu66, and Asp69 were found to be most significantly shifted with Met7 being known to be directly involved in DNA binding (Figure 5, panel c). Among the significantly shifted residues, Met7, Glu66, and Asp69 are in spatial proximity, whereas His29 is located in loop 1 of the HMG's major wing (Figure 5, panel c). The contribution of these residues to POM binding was investigated further by docking studies and was aided by comparison with solution structures of Sox17 (PDB: 2YUL), Sox5 (PDB: 1I11) and the DNA bound structure of Sox2 (PDB: 1GT0). Buried core residues like Trp13, Ala22, Lys27, and Ile33 mediating the stacking of helices 1 and 2 were least perturbed upon POM binding, suggesting that the structural integrity of the HMG domain is retained upon inhibitor binding (Supplementary Figure 1, panel a). Many of Sox2-HMG residues exhibited moderate chemical shift changes, suggesting global structural perturbation of Sox2 upon POM binding due to allosteric effects.[43,44]

Preferential Binding Site of the Dawson-POM on the Sox2-HMG Surface. To identify the site of interaction of the Dawson-POM with the Sox2-HMG, autodock searches were undertaken using the docking server methodology.[45,46] First, a blind docking search was set up such that the POM can explore the entire surface of a Sox2-HMG model derived from a crystal structure.[19] The second search was restrained to the area defined by the cluster of the residues Met7, Glu66, and Asp69 which were identified to be shifted from [^{15}N,^{1}H]-TROSY NMR. Both docking calculations identified a common binding mode indicating that this binding site is highly preferred by the POM. The binding pocket is formed by the C-terminus of helix-3 and the N-terminal region of the minor wing of the Sox2-HMG structure (Figure 6, panel a). Both shape and charge complementarities are favorable for ligand binding (Supplementary Figure 1, panel b). The negatively charged surface of POM can form many favorable electrostatic interactions when bound to Sox2, evident from the very low docking energy of −10.6 kcal/mol (Supplementary Figure 1, panel b). The positively charged side chains of Lys4, Arg5, Arg15, His63, and His67 can form hydrogen bonds or electrostatic interactions with the negatively charged oxygens of POM. The backbone amide of Lys4 forms an additional hydrogen bond with POM (Figure 6, panel a). In accordance with the docking studies, the positively charged residues Lys4, Arg5, and Arg15 exhibit moderate chemical shift changes, whereas His63 and His67 exhibit insignificant perturbation. Solvent accessibility analysis of apo-Sox2-HMG reveals that His63 and His67 are partially buried (13−30% exposure, Supplementary Figure 1, panel a) providing a likely reason for the lack of significant chemical perturbation for these residues. Glu66 of the POM binding cavity was most strongly shifted following POM addition (Figure 6, panel a). Although a protonated state of Glu66 could be envisaged to form a hydrogen bond with a terminal POM due to a slightly altered pH microenvironment, it is unlikely at the experimental conditions. Rather, the POM binding might repel Glu66 due to unfavorable electrostatic repulsion causing it to structurally reorient with respect to the apo-Sox2-HMG. Asp69 is a residue strongly perturbed in TROSY but is not present in the POM docking site. Asp69 is located in the C-terminal of helix 3, which is a region subject to inherent conformational changes due to protein flexibility as shown in NMR studies on apo Sox4 and Sox5.[47,48] Following DNA binding, however, the C-terminus is markedly rearranged to participate in the DNA interaction.[27] Thus, the pronounced perturbation detected for Asp69 likely

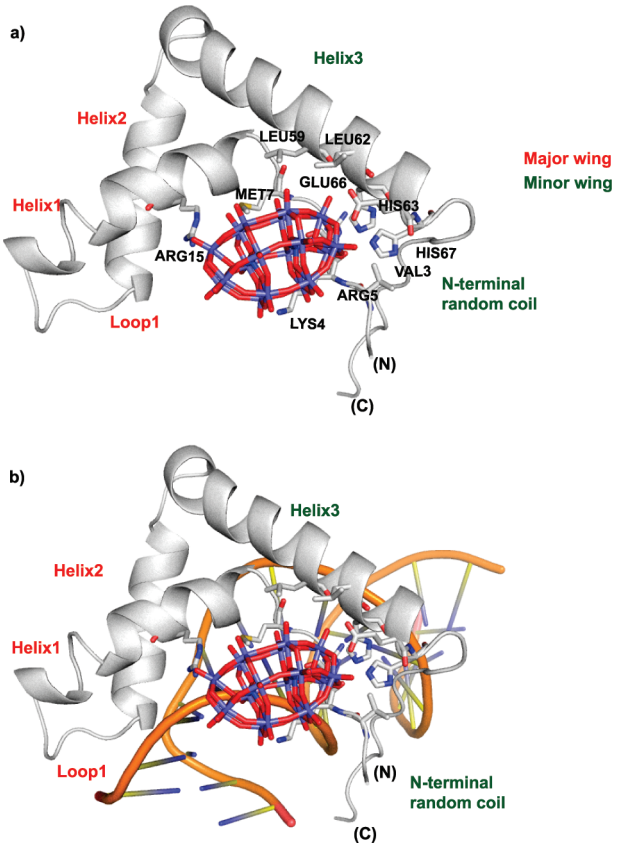

Figure 6. Sox2 Dawson-POM interactions at the docking site. (a) The lowest energy Sox2-HMG-POM complex structure from autodock searches shows that the POM is positioned within a pocket of the minor wing of Sox2-HMG. Lys4, Arg5, Arg15, His63, and His67 are involved in electrostatic or hydrogen bond interactions. Glu66 could donate hydrogen bonds in a protonated form. Leu52, Leu62, Met7, and Val3 shape the binding cavity. (b) Comparison of the docked model with the Sox2 X-ray structure (PDB: 1GT0) reveals that binding of POM would directly interfere with DNA binding due to charge repulsion.

illustrated the dynamics of this region and its structural adjustments accompanying molecular recognition events. The strongly perturbed His29 emanating from loop1 is another residue that is not located in the POM docking (Figure 5, panel c). This loop was found to exhibit the most pronounced Cα RMSD deviation within the helical core of the HMG domain when the DNA-bound Sox17 was compared with apo-Sox5 and Sox17 and also between individual structures from the apo-Sox5 NMR ensemble.[27] By inspecting the different conformers of the solution structure of Sox17 (PDB: 2YUL), it is evident that the N-terminal region of the minor wing is dynamic adopting conformations where the minor wing approaches loop1 indicating the potential of a cross-talk between the major and minor wings. The Sox2-HMG construct employed here contains an N-terminus extended by 13 amino acids as compared to the homologous Sox17 structure (PDB: 2YUL). Thus, it is conceivable that a longer dynamic Sox2 N-terminus would come into contact with His29 in loop1 due to conformational reorganization of the HMG wings induced by POM binding. In addition to charged amino acids, hydrophobic residues like Val3, Met7, Leu59, and Leu62 shape the cavity of the POM docking site (Figure 6, panel b). Consistently, Met7 exhibited a significant chemical shift in the TROSY experiment while Val3, Leu59, and Leu62 are moderately affected.

Together, NMR and docking studies suggest a model illustrating how the Dawson-POM brings about the inhibition of the Sox2-HMG DNA interaction. First, a comparison of the Sox2-POM docked structure with the X-ray structure of the ternary Oct1.Sox2.DNA complex (PDB: 1GT0) reveals that the binding of POM to this site would repel the phosphate backbone of DNA and compete with the positively charged residues in Sox2 (Figure 6, panel b). Second, the binding of POM could induce structural rearrangements of the N-terminal Sox2-HMG minor wing favoring a closed conformation. Together, the POM would occupy a site and cause structural rearrangements incompatible with DNA binding. An atomic structure of a Sox2-HMG/POM complex would provide valuable insights into the mechanism of POM inhibition. By analyzing a multiple sequence alignments it was observed that the bulk of the POM contacting residues are conserved within the Sox family (Supplementary Figure 1, panel c). We therefore tested whether the Dawson-POM can also inhibit the divergent Sox5, Sox7, and Sox17 proteins (Supplementary Table 2). Indeed, these experiments revealed a comparable reduction of the residual DNA binding activities for all tested Sox-HMG proteins. Thus, we propose the Dawson-POM as a potent lead scaffold for inhibiting the Sox family and that its selectivity could be fine-tuned by organic modifications.

Conclusion. The DNA binding domains of transcription factors have previously been considered too impervious to be tackled as drug targets, although upregulated transcription factors are a major cause of cancer and other diseases.[1,4,49] Here we identified a Dawson-POM as an unconventional but potent compound to inhibit the DNA binding activity of Sox2. The scaffold of the inorganic POMs has many favorable properties that could be fine-tuned to target the DNA binding domains of transcription factors. The mode of interaction of the Dawson-POM with the Sox2-HMG domain involves predominantly electrostatic interactions at the pocket just outside of the DNA binding region but still adequately positioned to compete with the negatively charged DNA backbone. To achieve selectivity to various classes of DNA binding domains, POMs can be modulated by derivatization with organic groups or by the modification of their charge distribution and dimensions.[31,50] Moreover, promising encapsulation techniques have been developed for POMs using starch nanoparticles as well as liposomes.[51,52] Such encapsulation techniques have been found to increase the efficacy of the delivery of the POMs to their target cell, resulting in significantly increased stability and bioactivity. In summary, the inhibitory mechanism of Sox2 by the Dawson-POM demonstrated here could eventually spawn the development of modified classes of POM-based drugs to specifically combat aberrant gene expression.

METHODS

Fluorescence Anisotropy Measurements. A fluorescence anisotropy assay was utilized to identify inhibitors of Sox2-HMG binding to its cognate DNA element. The 22bp fluorescein-labeled DNA element was based on a *cis*-regulatory element of the *CCND1* gene.[29] The assays were carried out in 384-well microplates (Corning NBS) in a buffer containing 10 mM Tris pH 8.0, 100 mM KCl, and 50 μM $ZnCl_2$. Fluorescence anisotropy was measured on a Spectramax M5 microplate reader (Molecular Devices) with excitation at 485 nm, emission at 525 nm, and a cutoff filter of 515 nm. The effect of different polyoxometalates on the residual DNA-binding activity of Sox2-HMG was determined by adding 1 μM of different POMs to a reaction mixture containing 85 nM Sox2-HMG and 1 nM fluorescein labeled CCND1 (~95% fraction bound condition). The experiments were carried out in triplicates, and the residual DNA binding activities at 1 μM POM are reported as a percentage of the controls.

Automated Anisotropy Fluorescence Based Screening. Liquid transfer steps were automated using the Caliper Life Sciences, Inc.'s Sciclone ALH 3000 Liquid Handler Workstation, and data were analyzed as outlined in the Supplementarty information.

NMR Spectroscopy and Data Processing. The NMR sample preparation is detailed in the Supporting Information. NMR experiments were performed on a Bruker AVANCE II 600 MHz NMR spectrometer equipped with four RF channels and a 5 mm z-gradient TCI cryoprobe. The spectra were collected at a regulated temperature of 298 K, and sweep widths for ^{1}H and ^{15}N were 9804 and 2412 Hz, respectively. The residual HDO resonance signal was suppressed with presaturation. A combination of experiments was used to derive the assignments of the backbone for Sox2-HMG. ^{1}H and ^{15}N resonances observed from the TROSY experiments were correlated with their corresponding inter- and intraresidue spin systems from 3D experiments, namely, HNCA, HNCACB, and CBCAcoNH, to sequentially correlate the amino acids. Data were processed using TopSpin 2.1, and the chemical shifts were referenced directly (^{1}H) to the frequency of DSS. Peak picking and spectral analysis was done using CARA.[53]

ASSOCIATED CONTENT

Supporting Information. Protein purification, EMSAs, proteolysis, thermo-fluor, screening data analysis and the docking studies. This material is available free of charge *via* the Internet at http://pubs.acs.org

AUTHOR INFORMATION

Corresponding Author
*E-mail: jauchr@gis.a-star.edu.sg.

ACKNOWLEDGMENT

We thank Christopher Wong for providing access to screening facilities. We are grateful to C. K-L. Ng, S. H. Choo, and N. BabuRajendran for assistance. The DTP, NIH kindly provided the mechanistic and challenge diversity libraries. This work is supported by the Agency for Science, Technology and Research (A*STAR) in Singapore and NRF2008NRF-CRP002-067 project 2 to K.P. We also thank Bernold Hasenknopf for reagents and critical advice.

REFERENCES

(1) Koehler, A. N. (2010) A complex task? Direct modulation of transcription factors with small molecules. *Curr. Opin. Chem. Biol. 14*, 331–340.

(2) Chan, L., Pineda, M., Heeres, J., Hergenrother, P., and Cunningham, B. (2008) A general method for discovering inhibitors of protein-DNA interactions using photonic crystal biosensors. *ACS Chem. Biol. 3*, 437–448.

(3) Darnell, J. E., Jr. (2002) Transcription factors as targets for cancer therapy. *Nat. Rev. Cancer 2*, 740–749.

(4) Berg, T. (2008) Inhibition of transcription factors with small organic molecules. *Curr. Opin. Chem. Biol. 12*, 464–471.

(5) Koehler, A. N., Shamji, A. F., and Schreiber, S. L. (2003) Discovery of an inhibitor of a transcription factor using small molecule microarrays and diversity-oriented synthesis. *J. Am. Chem. Soc. 125*, 8420–8421.

(6) Mao, C., Patterson, N., Cherian, M., Aninye, I., Zhang, C., Montoya, J., Cheng, J., Putt, K., Hergenrother, P., Wilson, E., Nardulli, A. Nordeen, S., and Shapiro, D. (2008) A new small molecule inhibitor of estrogen receptor alpha binding to estrogen response elements blocks estrogen-dependent growth of cancer cells. *J. Biol. Chem. 283*, 12819–12830.

(7) Rishi, V., Potter, T., Laudeman, J., Reinhart, R., Silvers, T., Selby, M., Stevenson, T., Krosky, P., Stephen, A., Acharya, A., Moll, J., Oh, W., Scudiero, D., Shoemaker, R., and Vinson, C. (2005) A high-throughput fluorescence-anisotropy screen that identifies small molecule inhibitors of the DNA binding of B-ZIP transcription factors. *Anal. Biochem. 340*, 259–271.

(8) Ng, P., Tang, Y., Knosp, W., Stadler, H., and Shaw, J. (2007) Synthesis of diverse lactam carboxamides leading to the discovery of a new transcription-factor inhibitor. *Angew. Chem., Int. Ed. 46*, 5352–5355.

(9) Anzellotti, A., Liu, Q., Bloemink, M., Scarsdale, J., and Farrell, N. (2006) Targeting retroviral Zn finger-DNA interactions: a small-molecule approach using the electrophilic nature of trans-platinum-nucleobase compounds. *Chem. Biol. 13*, 539–548.

(10) Wang, L., Yang, X., Zhang, X., Mihalic, K., Fan, Y., Xiao, W., Howard, O., Appella, E., Maynard, A., and Farrar, W. (2004) Suppression of breast cancer by chemical modulation of vulnerable zinc fingers in estrogen receptor. *Nat. Med. 10*, 40–47.

(11) Nickols, N. G., Jacobs, C. S., Farkas, M. E., and Dervan, P. B. (2007) Modulating hypoxia-inducible transcription by disrupting the HIF-1-DNA interface. *ACS Chem. Biol. 2*, 561–571.

(12) Lee, L. W., and Mapp, A. K. (2010) Transcriptional switches: chemical approaches to gene regulation. *J. Biol. Chem. 285*, 11033–11038.

(13) Ma, Y., Kurtyka, C. A., Boyapalle, S., Sung, S. S., Lawrence, H., Guida, W., and Cress, W. D. (2008) A small-molecule E2F inhibitor blocks growth in a melanoma culture model. *Cancer Res. 68*, 6292–6299.

(14) Dervan, P. B. (2001) Molecular recognition of DNA by small molecules. *Bioorg. Med. Chem. 9*, 2215–2235.

(15) Avilion, A. A., Nicolis, S. K., Pevny, L. H., Perez, L., Vivian, N., and Lovell-Badge, R. (2003) Multipotent cell lineages in early mouse development depend on SOX2 function. *Genes Dev. 17*, 126–140.

(16) Fong, H., Hohenstein, K. A., and Donovan, P. J. (2008) Regulation of self-renewal and pluripotency by Sox2 in human embryonic stem cells. *Stem Cells 26*, 1931–1938.

(17) Graham, V., Khudyakov, J., Ellis, P., and Pevny, L. (2003) SOX2 functions to maintain neural progenitor identity. *Neuron 39*, 749–765.

(18) Takahashi, K., and Yamanaka, S. (2006) Induction of pluripotent stem cells from mouse embryonic and adult fibroblast cultures by defined factors. *Cell 126*, 663–676.

(19) Remenyi, A., Lins, K., Nissen, L. J., Reinbold, R., Scholer, H. R., and Wilmanns, M. (2003) Crystal structure of a POU/HMG/DNA ternary complex suggests differential assembly of Oct4 and Sox2 on two enhancers. *Genes Dev. 17*, 2048–2059.

(20) Dong, C., Wilhelm, D., and Koopman, P. (2004) Sox genes and cancer. *Cytogenet. Genome Res. 105*, 442–447.

(21) Chen, Y., Shi, L., Zhang, L., Li, R., Liang, J., Yu, W., Sun, L., Yang, X., Wang, Y., Zhang, Y., and Shang, Y. (2008) The molecular mechanism governing the oncogenic potential of SOX2 in breast cancer. *J. Biol. Chem. 283*, 17969–17978.

(22) Bass, A. J., Watanabe, H., Mermel, C. H., Yu, S., Perner, S., Verhaak, R. G., Kim, S. Y., Wardwell, L., Tamayo, P., Gat-Viks, I., Ramos, A. H., Woo, M. S., Weir, B. A., Getz, G., Beroukhim, R., O'Kelly, M., Dutt, A., Rozenblatt-Rosen, O., Dziunycz, P., Komisarof, J., Chirieac, L. R., Lafargue, C. J., Scheble, V., Wilbertz, T., Ma, C., Rao, S., Nakagawa, H., Stairs, D. B., Lin, L., Giordano, T. J., Wagner, P., Minna, J. D., Gazdar, A. F., Zhu, C. Q., Brose, M. S., Cecconello, I., Jr, U. R., Marie, S. K., Dahl, O., Shivdasani, R. A., Tsao, M. S., Rubin, M. A., Wong, K. K., Regev, A., Hahn, W. C., Beer, D. G., Rustgi, A. K., and Meyerson, M. (2009) SOX2 is an amplified lineage-survival oncogene in lung and esophageal squamous cell carcinomas. *Nat. Genet. 41*, 1238–1242.

(23) Spisek, R., Kukreja, A., Chen, L. C., Matthews, P., Mazumder, A., Vesole, D., Jagannath, S., Zebroski, H. A., Simpson, A. J., Ritter, G., Durie, B., Crowley, J., Shaughnessy, J. D., Jr., Scanlan, M. J., Gure, A. O., Barlogie, B., and Dhodapkar, M. V. (2007) Frequent and specific immunity to the embryonal stem cell-associated antigen SOX2 in patients with monoclonal gammopathy. *J. Exp. Med. 204*, 831–840.

(24) Borowiak, M., Maehr, R., Chen, S., Chen, A. E., Tang, W., Fox, J. L., Schreiber, S. L., and Melton, D. A. (2009) Small molecules efficiently direct endodermal differentiation of mouse and human embryonic stem cells. *Cell Stem Cell 4*, 348–358.

(25) Boyer, L. A., Lee, T. I., Cole, M. F., Johnstone, S. E., Levine, S. S., Zucker, J. P., Guenther, M. G., Kumar, R. M., Murray, H. L., Jenner, R. G., Gifford, D. K., Melton, D. A., Jaenisch, R., and Young, R. A. (2005) Core transcriptional regulatory circuitry in human embryonic stem cells. *Cell 122*, 947–956.

(26) Werner, M. H., Huth, J. R., Gronenborn, A. M., and Clore, G. M. (1995) Molecular basis of human 46X,Y sex reversal revealed from the three-dimensional solution structure of the human SRY-DNA complex. *Cell 81*, 705–714.

(27) Palasingam, P., Jauch, R., Ng, C. K., and Kolatkar, P. R. (2009) The structure of Sox17 bound to DNA reveals a conserved bending topology but selective protein interaction platforms. *J. Mol. Biol. 388*, 619–630.

(28) Weiss, M. A. (2001) Floppy SOX: mutual induced fit in hmg (high-mobility group) box-DNA recognition. *Mol. Endocrinol. 15*, 353–362.

(29) Chen, Y., Shi, L., Zhang, L., Li, R., Liang, J., Yu, W., Sun, L., Yang, X., Wang, Y., Zhang, Y., and Shang, Y. (2008) The molecular mechanism governing the oncogenic potential of SOX2 in breast cancer. *J. Biol. Chem. 283*, 17969–17978.

(30) Michael Pope, A. M. (1994) *Polyoxometalates. From Platonic Solids to Anti-Retroviral Activity*, Kluwer Academic Publishers, Dordrecht, The Netherlands.

(31) Hasenknopf, B. (2005) Polyoxometalates: introduction to a class of inorganic compounds and their biomedical applications. *Front. Biosci. 10*, 275–287.

(32) Rhule, J. T., Hill, C. L., Judd, D. A., and Schinazi, R. F. (1998) Polyoxometalates in medicine. *Chem. Rev. 98*, 327–358.

(33) Moskovitz, B. L. (1988) Clinical trial of tolerance of HPA-23 in patients with acquired immune deficiency syndrome. *Antimicrob. Agents Chemother. 32*, 1300–1303.

(34) Herve, M., Sinoussi-Barre, F., Chermann, J., Herve, G., and Jasmin, C. (1983) Correlation between structure of polyoxotungstates and their inhibitory activity on polymerases. *Biochem. Biophys. Res. Commun. 116*, 222–229.

(35) Reinke, C. M., Drach, J. C., Shipman, C., Jr., and Weissbach, A. (1978) Differential inhibition of mammalian DNA polymerases alpha, beta and gamma and herpes simplex virus-induced DNA polymerase by the 5′-triphosphates of arabinosyladenine and arabinosylcytosine. *IARC Sci. Publ.* 999–1005.

(36) Sarafianos, S., Kortz, U., Pope, M., and Modak, M. (1996) Mechanism of polyoxometalate-mediated inactivation of DNA polymerases: an analysis with HIV-1 reverse transcriptase indicates specificity for the DNA-binding cleft. *Biochem. J. 319* (Pt 2), 619–626.

(37) Li, Y., He, Y., and Luo, Y. (2009) Crystal structure of an archaeal Rad51 homologue in complex with a metatungstate inhibitor. *Biochemistry 48*, 6805–6810.

(38) Prudent, R., Moucadel, V., Laudet, B., Barette, C., Lafanechere, L., Hasenknopf, B., Li, J., Bareyt, S., Lacote, E., Thorimbert, S., Malacria, M., Gouzerh, P., and Cochet, C. (2008) Identification of polyoxometalates as nanomolar noncompetitive inhibitors of protein kinase CK2. *Chem. Biol. 15*, 683–692.

(39) Learman, S., Kim, C., Stevens, N., Kim, S., Wojcik, E., and Walker, R. (2009) NSC 622124 inhibits human Eg5 and other kinesins via interaction with the conserved microtubule-binding site. *Biochemistry 48*, 1754–1762.

(40) Briand, L. E., Valle, G. M., and Thomas, H. J. (2002) Stability of the phospho-molybdic Dawson-type ion $[P_2Mo_{18}O_{62}]^{6-}$ in aqueous media. *J. Mater. Chem. 12*, 299–304.

(41) Xu, H. E., Rould, M. A., Xu, W., Epstein, J. A., Maas, R. L., and Pabo, C. O. (1999) Crystal structure of the human Pax6 paired domain-DNA complex reveals specific roles for the linker region and

carboxy-terminal subdomain in DNA binding. *Genes Dev. 13*, 1263–1275.

(42) Johnson, R., Samuel, J., Ng, C. K., Jauch, R., Stanton, L. W., and Wood, I. C. (2009) Evolution of the vertebrate gene regulatory network controlled by the transcriptional repressor REST. *Mol. Biol. Evol. 26*, 1491–1507.

(43) Gao, G., Williams, J. G., and Campbell, S. L. (2004) Protein-protein interaction analysis by nuclear magnetic resonance spectroscopy. *Methods Mol. Biol. 261*, 79–92.

(44) Akabayov, S. R., Biron, Z., Lamken, P., Piehler, J., and Anglister, J. (2010) NMR mapping of the IFNAR1-EC binding site on IFNalpha2 reveals allosteric changes in the IFNAR2-EC binding site. *Biochemistry 49*, 687–695.

(45) Bikadi, Z., and Hazai, E. (2009) Application of the PM6 semi-empirical method to modeling proteins enhances docking accuracy of AutoDock. *J. Cheminform. 1*, 15.

(46) Hazai, E., Kovacs, S., Demko, L., and Bikadi, Z. (2009) [DockingServer: molecular docking calculations online]. *Acta Pharm. Hung. 79*, 17–21.

(47) van Houte, L. P., Chuprina, V. P., van der Wetering, M., Boelens, R., Kaptein, R., and Clevers, H. (1995) Solution structure of the sequence-specific HMG box of the lymphocyte transcriptional activator Sox-4. *J. Biol. Chem. 270*, 30516–30524.

(48) Cary, P. D., Read, C. M., Davis, B., Driscoll, P. C., and Crane-Robinson, C. (2001) Solution structure and backbone dynamics of the DNA-binding domain of mouse Sox-5. *Protein Sci. 10*, 83–98.

(49) Rigby, A. C. (2009) Exploring novel chemical space through the use of computational and structural biology. *Comb. Chem. High Throughput Screening 12*, 927–928.

(50) Morris, G. M., Goodsell, D. S., Halliday, R. S., Huey, R., Hart, W. E., Belew, R. K., and Olson, A. J. (1998) Automated docking using a Lamarckian genetic algorithm and and empirical binding free energy function. *J. Comput. Chem. 19*, 1639–1662.

(51) Wang, X., Li, F., Liu, S., and Pope, M. T. (2005) New liposome-encapsulated-polyoxometalates: synthesis and antitumoral activity. *J. Inorg. Biochem. 99*, 452–457.

(52) Wang, X., Liu, J., and Pope, M. T. (2003) New polyoxometalate/starch nanomaterial: synthesis, characterization and antitumoral activity. *Dalton Trans.* 957–960.

(53) keller, R. (2004) *Optimizing the Process of Nuclear Magnetic Resonance Spectrum Analysis and Computer Aided Resonance Assignment*, Swiss Federal Institute of Technology (ETH), Zurich.